Check for updates

Electrifying the production of sustainable aviation fuel: the risks, economics, and environmental benefits of emerging pathways including CO_2†

R. Gary Grim, [iD] *[a] Dwarak Ravikumar,[a] Eric C. D. Tan, [iD] [a] Zhe Huang,[a] Jack R. Ferrell III, [iD] [a] Michael Resch, [iD] [a] Zhenglong Li,[b] Chirag Mevawala,[c] Steven D. Phillips,[c] Lesley Snowden-Swan,[c] Ling Tao [iD] [a] and Joshua A. Schaidle [iD] *[a]

Due to challenges related to weight and travel distance, the medium to long-haul aviation sector is expected to remain reliant on liquid hydrocarbon fuels into the foreseeable future, representing a persistent source of CO_2 emissions within the anthropogenic carbon cycle. As the world grapples with the environmental fallout from rising CO_2 emissions, a prevailing strategy to mitigate the impact of air travel is through the utilization of sustainable aviation fuels (SAF) produced from biogenic carbon sources such as fats, oils, greases, and biomass. However, with the demand for SAF expected to grow substantially in the coming decades, there is concern around the availability of these feedstocks at scale. Recent studies have proposed that this potential gap in supply could be closed by utilizing CO_2 as a complementary source of carbon combined with renewable electricity to drive the chemical transformation. In this study, a cross-cutting comparison of an emerging CO_2-to-SAF pathway with existing routes to SAF is performed, revealing the potential for CO_2-derived SAF to be competitive both in terms of costs and carbon intensity, further diversifying future options for SAF and providing a complementary option for the conversion of CO_2-to-SAF beyond the decades old methanol to olefins (MTO) and Fischer–Tropsch (FT) technologies. In addition, we discuss potential technical, market, and systems integration risks for the ultimate scale-up and commercialization of the pathway identified herein.

Broader context

As governments world-wide continue to explore options for reducing emissions across the global economy, it is becoming clearer that there is unlikely to be a "one-size-fits-all" solution, but rather a diversified portfolio of technologies and sustainable feedstocks will be needed. This paradigm is on display in the ongoing efforts to produce sustainable aviation fuels where recent projections indicate current conversion strategies, focusing on (wet) organic feedstocks such as biomass, wastes, animal fats, and oils, may be unable to satisfy the growing global demand, requiring alternative approaches. In this contribution we explore an emerging route to SAF involving front-end "power-to-liquids" (P2L) technologies whereby renewable electricity and carbon dioxide are used to produce SAF precursors in combination with secondary downstream conversion steps. Using a consistent basis of assumptions, we perform cross-cutting technoeconomic and life-cycle analyses to compare P2L CO_2-to-SAF technologies against existing SAF routes to highlight, on a like-for-like basis, the economic and environmental merits, R&D needs, and the risks associated with the scaling of these emerging technologies.

[a] *National Renewable Energy Laboratory, 15013 Denver W Pkwy, Golden, CO 80401, USA. E-mail: gary.grim@nrel.gov, joshua.schaidle@nrel.gov*

[b] *Oak Ridge National Laboratory, 1 Bethel Valley Rd, Oak Ridge, TN 37830, USA*

[c] *Pacific Northwest National Laboratory, 902 Battelle Blvd, Richland, WA 99354, USA*

Introduction

In the year 1903 humankind took flight for the first time, ushering in a new era for travel. Fast forward nearly 120 years and over 4.5 billion people are taking to the skies across 39 million flights each year.[1] Along with the rise in air travel has come substantial economic growth and globalization in which goods, people, and services can now reach all corners of the globe with an ease never before seen. However, increased access to air travel has not come without cost. Recent data finds
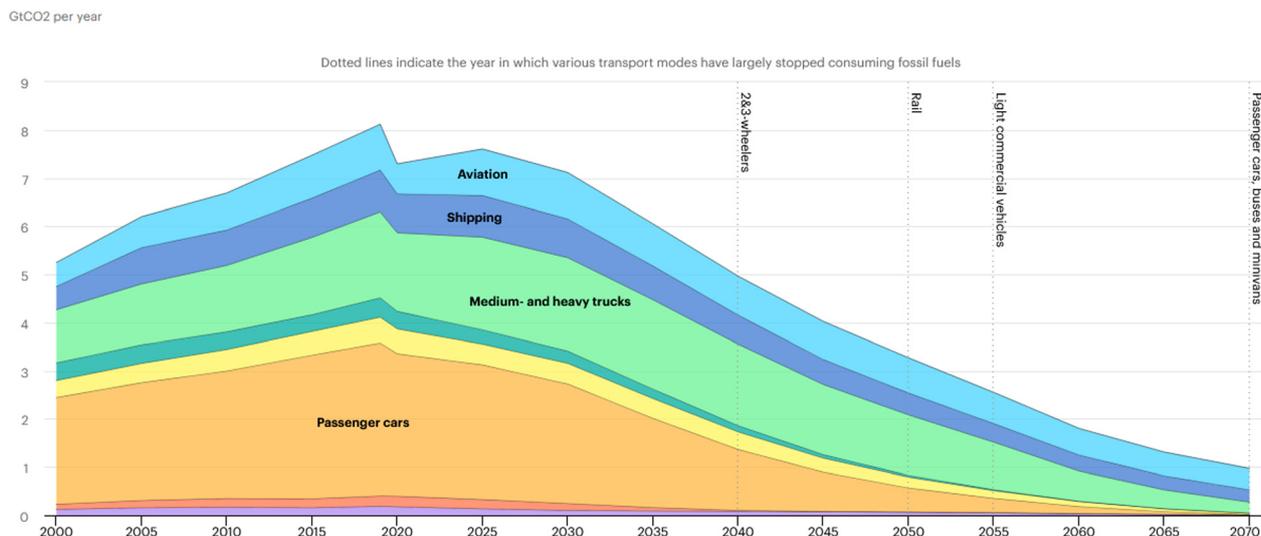
Fig. 1 Estimated global CO_2 emissions from the transportation sector in gigatonnes per year (2000–2070). Source: IEA, energy technology perspectives 2020, [6]

over 100 billion gallons of predominantly fossil-based jet fuel are consumed each year to power the global aviation sector, contributing to approximately 11% of all transportation-related CO_2 emissions and 3% of total anthropogenic CO_2 emissions.[2,3] Further, in addition to CO_2, combustion of fossil-derived jet fuel promotes SOx, NOx, particulate, and contrail formation in the upper atmosphere, which are believed to contribute to additional greenhouse warming of our planet.[4] With demand for jet fuel expected to more than double by 2050[5] and triple by 2070,[6] immediate efforts to decarbonize the aviation sector are needed to curtail rising emissions and avert the worst outcomes of climate change.

In other areas of the transportation sector, decarbonization efforts have begun to achieve some measures of success through direct electrification *via* renewable electricity and battery storage. For example, as shown in Fig. 1, the International Energy Agency (IEA) now predicts we will see a peak in global passenger car emissions (*i.e.*, gasoline consumption) around 2020, declining to zero by the year 2070. However, a comparable decrease in emissions is not forecasted for aviation. Aviation-related emissions are projected to continue rising during the 2020s and eventually overtake commercial trucking to become the largest source of transportation-related emissions by mid to late century. This resilience in medium to long-haul aviation emissions largely stems from the need for high density energy sources which, to date, cannot be met by battery systems and electricity directly, instead requiring the persistent use of energy-dense liquid fuels.

To minimize the environmental impacts associated with the combustion of jet fuel, recent efforts have focused on the development and commercialization of sustainable aviation fuels (SAF) derived from non-fossil feedstocks. To date, ASTM International has certified seven pathways to make SAF predominantly involving biomass, municipal solid waste (MSW), fats, oils, and greases (FOG), sugars, and alcohol feedstocks paired with established conversion technologies such as Fischer–Tropsch (FT), hydro-processed esters and fatty acids

(HEFA), and alcohol-to-jet (ATJ).[5] SAF offers two main advantages relative to conventional jet fuel in that (1) the upstream utilization of sustainably sourced feedstocks can significantly lower the carbon intensity (CI) of the SAF product and provide the potential for a near carbon-neutral pathway to fuels, and (2) SAF is considered to be cleaner burning due to reduced formation of particulates and other harmful side products.[4] However, the current focus on primarily organic feedstocks such as biomass and other plant and animal by-products, while a boon for sustainability, also presents a different set of challenges from the perspective of sourcing and supply logistics, scalability, cost, and land use. Whereas conventional jet fuel production is typically consolidated across a handful of oil-producing countries in large scale refineries at production rates of up to 100 000s bbl day^{-1} to leverage benefits of economies of scale and reduced cost, the lower energy density and dispersed nature of current SAF feedstocks means SAF production is likely to be more distributed and smaller in scale, requiring an estimated future 5000–7000 individual bio-refineries worldwide co-located with feedstock supply.[4] Combining these challenges with the anticipated future competition for sustainable sources of carbon, it is estimated that HEFA and other current bio-focused routes to SAF may only be able to meet approximately 50% of the global SAF demand by 2050.[4]

To expand the list of potential feedstocks beyond current options of biomass, FOG, MSW, *etc.*, and meet the additional 50% of projected global SAF demand, researchers are now looking to e-fuels where, in a process known as "power-to-liquids" (P2L), renewable electricity and/or electrolytic H_2 along with CO_2 are converted into intermediate SAF precursors or, in some cases, directly into drop-in SAF products. While comparably lower in technical maturity relative to some existing SAF pathways, the utilization of CO_2 offers a near limitless feedstock supply by taking advantage of carbon available in the anthropogenic carbon cycle, whilst simultaneously keeping virgin fossil carbon resources

locked away beneath the earth. P2L technologies are also suggested to offer additional potential benefits relative to conventional production in terms of enhancing renewable energy deployment through increased storage capabilities, providing more flexibility in deployment location, enhanced electrical grid stability, and lower SAF CI depending on the source of electricity.[7–10]

However, to fully quantify the benefits of P2L CO_2-to-SAF routes relative to other more established pathways, comparative techno-economic and life cycle analyses (TEA/LCA) are needed. While numerous TEA and LCA reports on SAF have been published previously, many focus on single conversion technologies and/or involve only biomass, FOG, or MSW feedstocks.[11–17] With P2L CO_2-derived SAF expected to comprise >50% of future global SAF supply, end-to-end analyses for P2L CO_2-to-SAF conversion with renewable electricity are critically needed and are largely absent in the current literature. A notable exception is the work of Schmidt *et al.*, in which P2L CO_2 conversion through existing methanol-to-olefins (MTO) and FT pathways was studied.[10] In this study, we fill this critical knowledge gap in three ways. First, expanding on the work from Schmidt, we look beyond the decades-old FT and MTO chemistries and identify, model, and analyze an emerging hybrid pathway for CO_2-to-SAF including electro-, bio-, and thermo-chemistry. Second, using fully integrated Aspen Plus process models informed from the most current publicly available data and patents, we calculate the minimum jet fuel selling price (MJSP) and CI of CO_2-derived SAF and provide a comparison with other notable SAF production routes. By using a consistent basis of assumptions across technologies, this cross-cutting analysis provides a like-for-like analysis of SAF production routes and clearly establishes the challenges and opportunities for CO_2-to-SAF relative to existing routes. Lastly, as with any new technology, there will be risks to scale-up and commercialization. Herein, we identify potential technical, market, and systems integration risks relevant to the scale-up and commercialization of CO_2-to-SAF pathways and propose key

geographic and site-specific metrics relevant to early market adopters.

Methodology

Description of CO_2-to-SAF pathway

In the studied CO_2-to-SAF pathway, it is assumed that SAF is produced *via* a three-step process, shown in Fig. 2, involving an electrolysis front-end to produce carbon monoxide (CO), a biological syngas fermentation stage to produce an ethanol intermediate, and a thermocatalytic ethanol upgrading step to produce the final SAF product. In this study we examine two cases for electrolysis, a low-temperature anion-exchange membrane (AEM) electrolyzer and high-temperature solid oxide electrolyzer cell (SOEC). We acknowledge that there are many potential pathways to produce SAF from CO_2, such as MTO and FT noted earlier, as well as *via* the direct conversion of C_{4+} alcohols.[18,19] We elected to model the three aforementioned steps as they (1) represent an emerging pathway of moderate technical maturity with a clear path towards commercialization, (2) utilize bioethanol which represents one of the largest sources of sustainable carbon in the United States, and (3) are compatible with P2L. The assumptions for each conversion step are discussed in detail below. It should be noted that the input values and assumptions for each conversion step were selected from publicly available data which were individually vetted by subject matter experts and are intended to provide a snapshot of the current state-of-technology for each respective process. The results presented in this report are specific only to the cases modeled herein and may not fully characterize and/or reflect the potential of other CO_2-to-SAF pathways.

Low-temperature electrolysis (LTE). In the first case which assumes the use of an LTE front-end, the incoming CO_2 feed is electrochemically reduced to CO and O_2 following eqn (1). While prior studies have shown proof of concept for the electroreduction of CO_2 to CO,[20–22] most have not demonstrated commercially relevant technical metrics nor reported
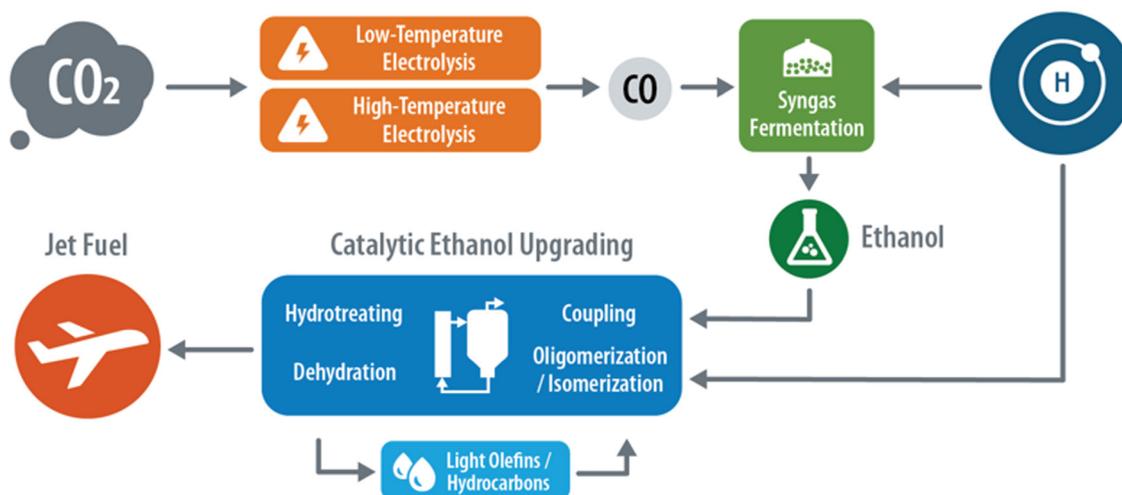

Fig. 2 Block flow diagram of the modelled pathway for CO_2-to-SAF.

4800 | *Energy Environ. Sci.*, 2022, **15**, 4798–4812

This journal is © The Royal Society of Chemistry 2022

Table 1 Technical assumptions for CO_2-to-SAF

| Parameter	Value	Ref.
Low-temperature electrolysis		
Whole cell voltage (V)	3.0	23
FE (%, CO)	98	23
Current density (mA cm^{-2})	200	23
Stability (h)	>3800	23
Single-pass CO_2 conversion (%)	43	23 and 28
Temperature (°C)	50	23
Total system cost ($ m^{-2})	19 739	29
Stack fraction (–)	0.74	29
BOP fraction (–)	0.26	29
Replacement interval (years)	3	29
Replacement cost ($)	15% stack	29
High-temperature electrolysis		
Whole cell voltage (V)	1.44	26
FE (%, CO)	99.5	24
Current density (mA cm^{-2})	772	24
Stability (h)	>7000	24 and 26
Single-pass CO_2 conversion (%)	50	30
Temperature (°C)	750	24 and 26
Total system cost ($ m^{-2})	7829	29
Stack fraction (–)	0.30	29
BOP fraction (–)	0.70	29
Replacement interval (years)	4	29
Replacement cost ($)	30% stack	29
Syn-gas fermentation		
Ethanol productivity (g EtOH L^{-1} d^{-1})	195	31
Ethanol selectivity (%)	95	32
CO Single-pass conversion (%)	95	32
Product titer (g EtOH L^{-1})	60	33
Bioreactor temperature (°C)	37	31
Bioreactor temperature (bara)	1–6	31
Media recycle (%)	80	32
Co-product selectivity		
Biomass/solids (%)	<2%	32
2,3-Butanediol (%)	<2%	32
Acetic acid (%)	<2%	32
Thermocatalytic ethanol to jet		
EtOH to light olefins		
Ethanol conversion	97	34
Carbon selectivity to olefins	81	34
Carbon selectivity to oxygenates	10	34
Carbon selectivity to paraffins		34
Catalyst	Ag–ZrO$_2$/silica	34
Temperature (°C)	325	34
Pressure (bara)	10	34
WHSV (h^{-1})	1.5	34
Oligomerization		
Single pass conversion (%)	65	35
Selectivity to C$_{9+}$ olefins, single pass (%)	66	35
Catalyst	HZSM-5	35
Temperature (°C)	225	35
Pressure (bara)	23	35
WHSV (h^{-1})	0.46	35
Hydrogenation		
Catalyst	Pd on alumina	—
Temperature (°C)	300	—
Pressure (bara)	21	—
WHSV (h^{-1})	5	—

system stability greater than on the order of 10s of hours. One of the highest performing systems amongst the literature to date with a reported stability of over 3800 hours is an AEM membrane electrode assembly (MEA) under development by Dioxide Materials.[23] CO_2 is reduced over an Ag electrocatalyst with a surface area of 5 cm^2 reaching both high current density and selectivity to CO while maintaining high stability. The technical metrics and other associated assumptions for LTE, as well as the other comprising conversion steps, are shown in Table 1.

$$CO_2 + H_2O + 2e^- \rightarrow CO + 2OH^- \qquad (1)$$

High-temperature electrolysis (HTE). In a second case, we examine the impact of replacing the LTE front-end with a high-temperature SOEC. Compared to LTE, HTE reduction of CO_2-to-CO offers a higher technology readiness level (TRL) process which has reached the pilot/pre-commercial stage by several companies such as Haldor-Topsoe and Siemens.[24,25] In addition to being of higher TRL, HTE processes are of interest based on the potential to operate with higher efficiency, at lower voltages, and with greater stability compared to LTE systems.[26] However, a trade-off is the requirement of much higher operating temperatures on the order of 550–850 °C[26,27] which, depending on the source of heat, could negatively impact the carbon footprint of the product and/or net process efficiency. In this work, the Haldor-Topsoe CO_2-to-CO experimental data was selected due to the exceptional reported stability showing stable operation over 7000 hours tested.[24,26]

Syngas fermentation. The intermediate CO product generated in the initial electrolysis stage, along with any unconverted CO_2, is then mixed downstream with a sustainable H_2 source creating a syngas mixture at a ratio of approximately 5 : 1 : 1 H_2 : CO : CO_2. Because H_2O electrolysis is of high TRL and is being explored commercially,[36] this step is not modelled explicitly, but rather treated as an operating expense. Further, with the goal of producing fuels with minimal CI, we assume the H_2 used within the study is from renewable sources only and does not rely on fossil feedstocks (e.g., steam methane reforming or grid electricity mix). The mixture of gases is fed to a fermenter to produce ethanol following the reaction shown in eqn (2).[37] The microbial productivity, selectivity, and conversion parameters are based on a proprietary anaerobic bacterium developed by LanzaTech, which has demonstrated compatibility across a range of H_2, CO, and CO_2 ratios.[31] The LanzaTech process was selected for this conversion stage as it has commercially demonstrated the syngas to ethanol process at a large scale from steel mill waste gas, representing a high TRL option to produce ethanol.[38]

$$5H_2 + CO + CO_2 \rightarrow C_2H_5OH + 2H_2O \qquad (2)$$
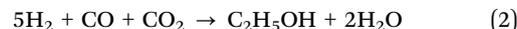
Thermocatalytic ethanol catalytic conversion. The final ethanol-to-SAF conversion step is based on the latest published research from Pacific Northwest National Laboratory (PNNL) following the three-step catalytic process shown in Fig. 2 involving ethanol dehydration to 1-butene in a single step, oligomerization, and hydrotreating stages with internal recycle loops to produce a jet fuel product (full PFD provided in Fig. S1, ESI†). The single-step ethanol to n-butene catalytic process has been developed and patented by PNNL and is at a TRL of 3–4 (U.S. Patent 10647622 issued 5/12/20 and U.S. Patent 11046623 issued 6/29/21). The downstream unit operations are TRL 8 or 9 and commonly used

This journal is © The Royal Society of Chemistry 2022

Energy Environ. Sci., 2022, **15**, 4798–4812 | **4801**

in refinery operations. See ESI,† for more details on process operating conditions.

Techno-economic analysis methodology

To model the end-to-end CO_2 to SAF process, a fully integrated Aspen Plus model was developed based on the CO_2-to-SAF scheme shown in Fig. 2. The design and technical parameters used within each conversion step (*e.g.*, LTE, HTE, fermentation, thermocatalysis) were chosen to represent the current state of technology for each of the respective processes based on demonstrated process stability, TRL, and input from subject matter experts. All values and assumptions were pulled from publicly available literature.

Process scale was based on an incoming flowrate of $\sim$52 000 kg h^{-1} of pure CO_2, equivalent to the off-gas of a $\sim$136 MMgal EtOH per year biorefinery. Mass and energy flowrates calculated from Aspen Plus were used to size and cost all major capital equipment. Unit costs for capital equipment were based on supplier quotes where available. In the absence of supplier data, Aspen Capital Cost Estimator (ACCE) was used. Equipment unit costs were typically scaled using an exponent term of 0.6, except in the case of the electrolyzers, which were scaled using a term of 1.0 based on similar PEM H_2O electrolyzer systems.[29,39] The material and energy flows along with capital cost information were input into a discounted cash flow rate of return economic model to calculate a minimum jet fuel selling price (MJSP) which corresponds to the minimum price that the SAF must sell for to generate a net present value of zero for a 10% internal rate of return. All costs are adjusted to 2016 United States dollars (2016$USD).

The economic and market assumptions applied in this study fall under one of three scenarios: conservative, optimistic, and aggressive. Our conservative economic assumptions represent values currently obtainable if a project were to be deployed today; however, acknowledging the likelihood for a more favorable future environment, we also consider an optimistic and an aggressive case as shown in Table 2. The optimistic market scenario reflects near-term future opportunities provided by falling renewable energy costs while keeping the current technology-specific assumptions from Table 1. The aggressive market case reflects very optimistic economic assumptions for future deployment coupled with moderate technological improvements across the comparably lower TRL electrolysis conversion steps, specifically related to metrics such as cell voltage, current density, and capital cost. Several of the most aggressive assumptions are aligned with strategic areas of interest, such as the U.S. Department of Energy's 2031 "Earthshot" goal of $1.00 per kg H_2.[40] All other TEA assumptions can be found in Table S1 (ESI†).

Life cycle analysis methodology

In this study we define the CO_2-to-SAF system boundary for LCA to include four stages highlighted in Fig. 3: (1) the capture and purification of the CO_2 feedstock, (2) the conversion of CO_2-to-SAF, (3) the transportation and storage of SAF, and (4) the final combustion of SAF. The first three steps, commonly referred to

Table 2 Financial scenarios

Economic parameters	Assumed basis
Conservative market case	
H_2 price[a] ($ kg^{-1})	4.50
CO_2 price ($ tonne^{-1})	40
Electricity price ($ kW h^{-1})	0.068
Optimistic market case	
H_2 price[a] ($ kg^{-1})	2.00
CO_2 price ($ tonne^{-1})	25
Electricity price ($ kW h^{-1})	0.02
Aggressive market case (+technological improvements)	
H_2 price[a] ($ kg^{-1})	1.00
CO_2 price ($ tonne^{-1})	0
Electricity price ($ kW h^{-1})	0.01
LTE voltage (V)	2.5
LTE current density (mA cm^{-2})	1000
LTE replacement interval (years)	7
LTE capital cost ($ m^{-2})	10 000
HTE voltage (V)	1.0
HTE current density (mA cm^{-2})	2000
HTE replacement interval (years)	7
HTE capital cost ($ m^{-2})	5000
HTE replacement cost ($)	15% stack

[a] Assumes electrolytic H_2 production.

as "well to pump" (WTP) emissions, are explicitly calculated in this work, whereas the final "pump to wake" (PTWa) step is considered constant and independent of the upstream technology and a value of 72.88 gCO_2e per MJ is applied directly from the Argonne National Laboratory GREET model.[41]

For the capture and purification of CO_2, a variety of ad- and absorption technologies are available across the many possible sources of CO_2. Due to the wide range in purity, concentration, and capture methods, the first key LCA assumption is around the CI of acquiring the CO_2 feedstock. In this study, we consider six possible sources of CO_2: (1) a bioethanol plant, (2) a cement plant, (3) a natural gas combined cycle (NGCC) power plant, and (4–6) three direct air capture (DAC) strategies including an industry average approach, vacuum temperature-swing adsorption (VTS), or hydroxide-based sorbents. Herein the classification of the CO_2 (*e.g.*, biogenic *vs.* fossil) was not explicitly accounted for and it was assumed that all captured CO_2 would have otherwise either been emitted to the atmosphere or, in the case of DAC, remained in the atmosphere.

To calculate the CI associated with the capture step from each point source, our base case assumption was to apply the average estimated energy intensity and associated energy emissions factors as reported by von der Assen *et al.*[42] and other literature sources for DAC.[43,44] These data assume the use of primarily grid electricity and/or fossil energy which is representative of how such processes are conducted today. Acknowledging the evolving energy landscape, we also add two comparison cases of CO_2 capture with DAC paired with renewable electricity (denoted below as RE) to show the potential for future emissions reductions through increased penetration of renewables and technology advancements. Across all cases, the calculated CI for sourcing CO_2 ranged from 0–0.53 kg CO_2e emitted per kg CO_2 captured, as shown in Table 3 depending on the source of

4802 | *Energy Environ. Sci.*, 2022, **15**, 4798–4812
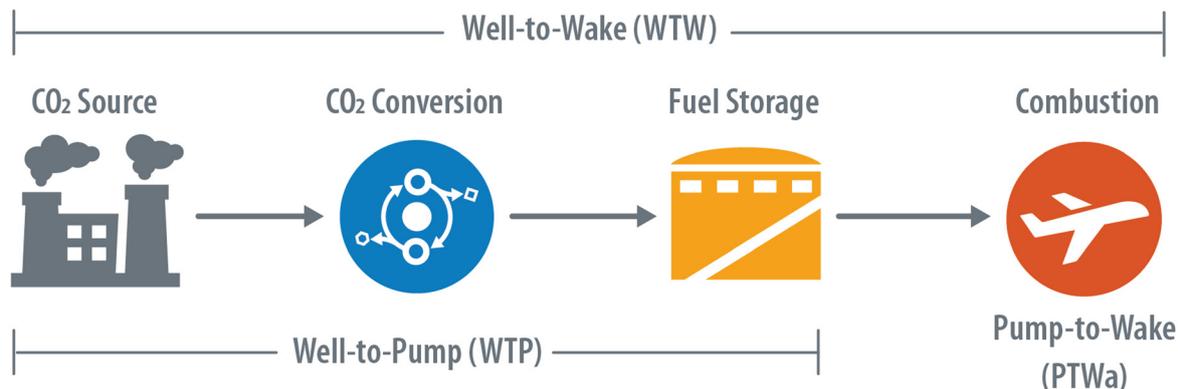
This journal is © The Royal Society of Chemistry 2022

Fig. 3 Life cycle analysis system boundary.

CO_2, carbon footprint of the energy source, and compression. For more information on assumptions see Tables S2–S5 (ESI†).

To calculate the greenhouse gas emissions associated with the CO_2-to-SAF conversion stage, we tabulate the major process inputs and outputs derived from the Aspen Plus model in a life cycle inventory table. Multiplying these major mass and energy flows by their associated emissions factor yields the total CO_2e emission rates for the process. Note herein we consider two primary data sources for emissions factors, the GREET database and the commercial LCA platform SimaPro which uses the EcoInvent database, when available. A major difference between the two platforms as it relates to P2L LCA is in the handling of renewable electricity emissions.

GREET assumes an emissions factor of 0 for renewable electricity (and renewable H_2) by default, whereas SimaPro and other literature sources[45,46] assigns a small but non-negligible value to renewable electricity generation to account for the upstream manufacturing, maintenance, and operation. Due to the high energy demands of P2L conversion, we only consider the use of renewable electricity for the conversion stage(s) and consequently, this small difference in carbon accounting for renewable electricity generation can have a significant impact on the final CI number. We report both data sets for full transparency with and without compression to 10 MPa to capture both bolt-on and centralized utilization

requiring feedstock transport. The life cycle inventory, complete list of emissions factors, and carbon intensity calculations are provided in Tables S6–S8 (ESI†).

Results and discussion

Life cycle analysis

Multiplying the major mass and energy flows of the CO_2-to-SAF model by their associated emissions factors yields the total hourly CO_2 equivalent (CO_2e) flow (provided in Table S8, ESI†). The total CO_2e flow normalized by the energy output in the SAF product yields CI in terms of gCO_2e per MJ. In Table 4, we show that depending on the source of CO_2 and the assumptions in emissions factors for renewable energy (*i.e.*, GREET *vs.* SimaPro), the CI for the default modeled CO_2-to-SAF process (LTE case) can range from as low as ~ 1 gCO_2e per MJ to as high as 61 gCO_2e per MJ.

These results highlight that the impact of selecting a CO_2 source extends beyond a simple difference in the raw input feedstock cost; rather, the concentration and purity of the source, and thus, by extension the assumptions around the energy intensity of the capture and purification step can dramatically impact the CI of the final SAF product. As shown in Tables 3 and 4, in some cases such as the most dilute CO_2 sources, over 50% of the total CO_2 consumed for use as a feedstock may be remitted during the capture step (on a net basis) due to high energy intensity and/or the associated emissions of sourcing the feedstock, increasing the final CI for SAF. Consequently, in an environment where making fuels with the lowest CI is becoming increasingly valued, both socially and from the perspective of qualifying for policy incentives, these data indicate the highest purity (*i.e.*, lowest energy intensive) CO_2 sources are likely to be highly coveted for early adopters as they can offer a greater reduction in CI relative to more dilute sources (*i.e.*, more energy intensive) shown in Fig. 4.

To minimize this disparity, research and development into conversion strategies that are compatible with dilute CO_2 streams and/or involve combined reactive capture + conversion[47] is warranted to reduce the energy burden on the upstream CO_2 collection stage(s). Further, reducing the CI of the energy used for CO_2

Table 3 Emissions factors for CO_2 capture and purification by source (data compiled from von der Assen *et al.*[42])

CO_2 source	Emissions factor (kg CO_2e per kg CO_2 captured)	Emissions factor @ 10 MPa (kg CO_2e per kg CO_2 captured)
DAC (Avg + FE Blend)[a]	0.48	0.53
DAC (Hydroxide + RE)[b]	0.08	0.14
DAC (VTS + RE)[c]	0.06	0.12
Cement[d]	0.29	0.35
NGCC[d]	0.16	0.21
Bioethanol[d]	0.0	0.05

[a] Average energy intensity for DAC systems using fossil/grid energy.[42] [b] Hydroxide-based DAC technology with renewable energy.[43] [c] Vacuum temperature-swing technology with renewable energy.[44] [d] Assumes grid electricity/fossil energy usage.[42]

This journal is © The Royal Society of Chemistry 2022

Energy Environ. Sci., 2022, **15**, 4798–4812 | **4803**

Table 4 SAF CI values for P2L CO$_2$-to-SAF (LTE case) by CO$_2$ source and emissions assumptions

CO$_2$ source	CI-GREET (gCO$_2$e per MJ)	CI-SimaPro (gCO$_2$e per MJ)
Bioethanol	1	21
Bioethanol (10 MPa)	5	25
Cement	24	44
Cement (10 MPa)	28	48
NGCC	13	33
NGCC (10 MPa)	17	37
DAC (VTS + RE)[a]	6	26
DAC (VTS + RE, 10 MPa)	10	30
DAC (Hydroxide + RE)[b]	7	27
DAC (Hydroxide + RE, 10 MPa)	12	31
DAC (Avg + FE)[c]	37	57
DAC (Avg + FE, 10 MPa)	42	61

[a] Vacuum temperature-swing technology with renewable energy.[44] [b] Hydroxide-based DAC technology with renewable energy.[43] [c] Average energy intensity for DAC systems using fossil/grid energy.[42]

capture by implementing a higher fraction of renewables will also serve to significantly lower the overall CI, as shown by the VTS and hydroxide DAC cases which assumed the use of renewable energy only.

With electricity being the major energy input for P2L processes, the results of the LCA also highlight another key finding with respect to how renewable electricity emissions are modeled and the implications for cross-comparing technologies on a like-for-like basis. Specifically, in the GREET model the emissions associated with renewable electricity and H$_2$ produced from green electricity sources are assumed as zero by default. Conversely, the EcoInvent database in the commercial LCA platform SimaPro as well as other literature sources[45,46] attribute a small amount of emissions to the manufacturing and operation of renewable energy infrastructure. Our data in Table 4 shows that for an identical set of process data these differences in accounting of renewable electricity emissions, in this case related to wind-derived electricity, contributes to a difference in ~20 gCO$_2$e per MJ to the SAF CI (LTE case) between the two methodologies, while keeping all other assumptions

constant. Considering both methodologies are widely used in scientific literature, harmonizing these assumptions, maintaining transparency, and using consistent reporting methods will be critical to progressing the field further as the prevalence of reporting CI becomes more commonplace in scientific literature.

In Fig. 4 we provide a comparison of P2L CO$_2$-to-SAF CI values against four ASTM-International certified SAF pathways and two pathways to conventional jet fuel evaluated using GREET methodology and electricity assumptions.[48] These data show that across all CO$_2$ sources considered, the LTE CO$_2$-to-SAF pathway can offer an approximately 50–94% reduction in CI relative to conventional jet fuel production (84 gCO$_2$e per MJ) depending on the source of CO$_2$.[41] Further, the LTE CO$_2$-to-SAF CI is in general in line with and/or lower than the shown ASTM-certified SAF pathways.

While all SAF pathways included herein represent an improvement in CI relative to the established fossil pathways, the difference in calculated CI becomes significant when considering incentives and credits where the monetary value is typically linked to the CI and GHG reduction potential. For instance, using California's low-carbon fuel standard (LCFS) as an example, SAF with a CI value of 42 gCO$_2$e per MJ (average DAC CO$_2$ source) would qualify for a $0.94 per gallon gasoline equivalent (GGE) incentive based on the price of the underlying credit (assumed here as $171 per ton), whereas at a CI of 5 gCO$_2$e per MJ (bioethanol CO$_2$ source), the same incentive increases in value by 78% to approximately $1.67 per GGE.[49] Additionally, recently passed legislation in the United States further widens the gap in economic incentives for low CI fuels. In the 2022 "Inflation Reduction Act" (IRA),[50] an additional $1.25 per gal incentive is provided for qualifying SAF pathways showing >50% reduction in CI relative to conventional jet fuel. This incentive is increased an additional $0.01 per gal for each percent reduction in CI above 50%, further benefiting the top performing pathways with the lowest CI. Between just these two credits, the LCFS and IRA, we show that the difference in the monetary value of these credits for our modelled cases (e.g., CI of 42 and CI of 5) could be as wide as
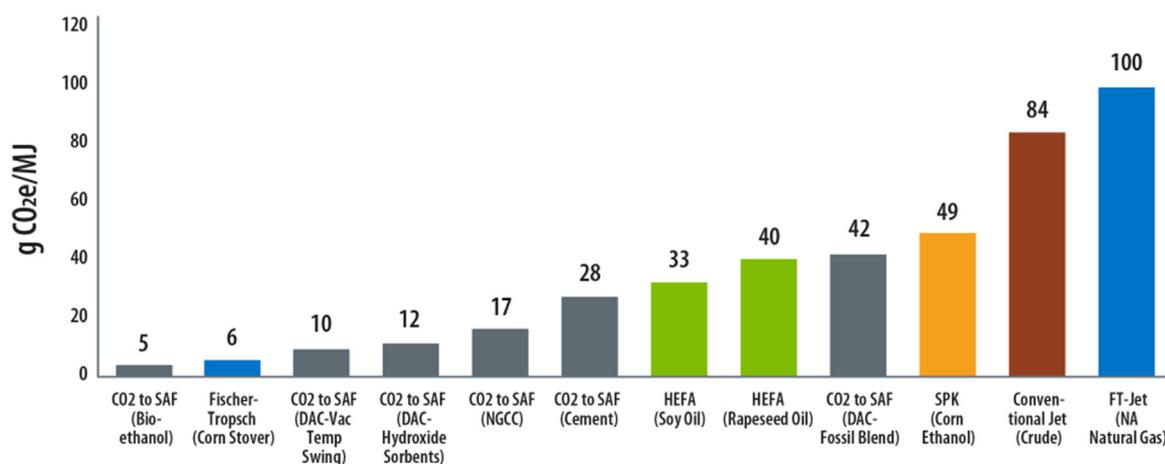

Fig. 4 Comparison of WTWa CI values across SAF pathways using the GREET methodology assuming compression to 10 MPa. Blue = Fischer–Tropsch, Grey = CO$_2$ utilization technologies, Green = HEFA, Orange = SPK, Red = conventional. All non-CO$_2$ routes to SAF sourced from GREET.[41,48] DAC VTS and DAC Hydroxide cases assume the use of renewable energy.

4804 | Energy Environ. Sci., 2022, **15**, 4798–4812

This journal is © The Royal Society of Chemistry 2022

$1.17 per GGE in total, which stands to strongly incentivize those pathways with the lowest CI (*e.g.*, high-purity CO_2 sources) and encourage integration with renewable electricity, especially for energy intensive capture and purification of dilute CO_2 sources. For more details and examples of incentive calculations, see ESI.†

Techno-economic analysis and minimum jet selling price

In Table 5, the calculated MJSP is presented for both the LTE and HTE P2L CO_2-to-SAF cases. We show that before the application of any credits or incentives, the MJSP under the conservative economic assumptions falls in the range of $7.49–10.49 per GGE, several multiples higher than that of the trailing 10 year U.S. jet fuel range. However, as more favorable market and technological assumptions are applied in the "optimistic market" and "aggressive market + tech" scenarios defined in Table 2, we find that the MJSPs are reduced substantially to the range of $3.97–6.45 per GGE under optimistic economic assumptions, and $2.25–2.53 per GGE, under the most aggressive economic assumptions with moderate technological improvements.

The major contributors to MJSP across the two studied cases under the conservative economic assumptions are provided in Fig. 5, showing that independent of the specific pathway, the number one cost driver impacting process economics is input electricity cost, as accounted for both directly in the CO_2 electrolysis step (BOP utilities) and indirectly for the H_2 generation step (H_2 electrolysis).

These data indicate, as discussed above, the economic viability of CO_2-to-SAF processes will be inextricably linked to available electricity price and maintaining a low-cost, high-capacity factor source of electricity will be crucial to the commercial success of P2L CO_2-to-SAF. Second to electricity price, we find the next largest contributor to MJSP is the process CAPEX, primarily due to the high capital intensity of the low and high temperature electrolyzers. In comparing the two pathways within the conservative market scenario, we show that the CAPEX contribution is significantly larger in the LTE case adding $2.90 per GGE to the MJSP compared to only $0.86 per GGE in the alternative HTE case. This difference stems from the higher assumed unit cost for low temperature electrolyzers

of $19 739 per m^2 (*versus* $7830 per m^2 for HTE) combined with the lower operating current densities, which necessitates more surface area and consequently larger systems. Additionally, due to the lack of longer duration stability testing of electrolyzers in a commercial setting, both electrolysis systems are modeled with relatively short replacement frequencies (3–4 years), which also contribute to the overall production cost as well as charges related to the depreciation of the high overall cost of capital. It is anticipated that as supply chains grow and economies of scale are leveraged, these capital costs will begin to fall; however, at this time the electrolyzer capital costs are major burdens on total plant costs. These results highlight over the near term and until R&D on the LTE systems lowers unit cost and raises operating current density, economic gains may be seen by using HTE systems for converting CO_2 to CO on the upstream portion of the process. However, high temperature electrolysis systems will require significant heat input which could be a detriment to deployment depending upon fuel source, location constraints, and availability at low cost.

Relative to the moving 10-year average U.S. jet fuel spot price of approximately $1.89 per GGE,[59] these data show that in the absence of policy-driven incentives, the two modeled CO_2-to-SAF cases show an average calculated price approximately 4.75× higher than that of fossil jet fuel under the conservative economic scenario. When compared to other pathways to produce SAF which are estimated to range from $1.26–13.30 per GGE depending on feedstock and conversion technology, we show in Fig. 6 that under conservative assumptions P2L CO_2-to-SAF currently falls on the upper end of this range and on the mid- to low-end of the range when optimistic and aggressive assumptions are applied. The economic competitiveness of CO_2-to-SAF could be further enhanced if policy incentives are considered, as discussed above, the potential for a lower CI final product can contribute to larger subsidies and credits to help offset any higher costs.

Energy efficiency for CO_2-to-SAF

The energy inputs and outputs for the as-modeled CO_2-to-SAF process fall across five categories: (1) CO_2 capture, (2) CO_2

Table 5 Techno-economic results for CO_2-to-SAF pathways (without incentives)

	MJSP ($ per GGE)
LTE case (conservative)	10.49
LTE case (optimistic)	6.45
LTE case (aggressive + tech)	2.53
HTE case (conservative)	7.49
HTE case (optimistic)	3.97
HTE case (aggressive + tech)	2.25
Estimated SAF production cost[a]	1.26–13.30
2011–2021 U.S. Jet spot price range[b]	0.55–2.97

[a] Data reflects current cost estimates across major SAF pathways based on ref. 51–58. [b] EIA U.S. Gulf Coast Kerosene-Type Jet Fuel Spot Price FOB.[59]
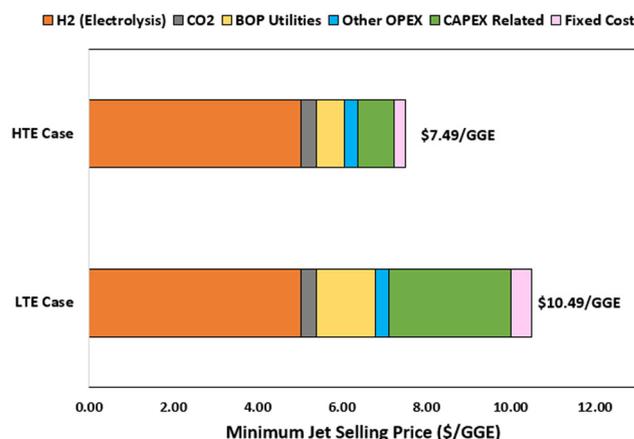

Fig. 5 Cost breakdown of the CO_2-to-SAF pathway (no incentives, conservative market scenario).

This journal is © The Royal Society of Chemistry 2022

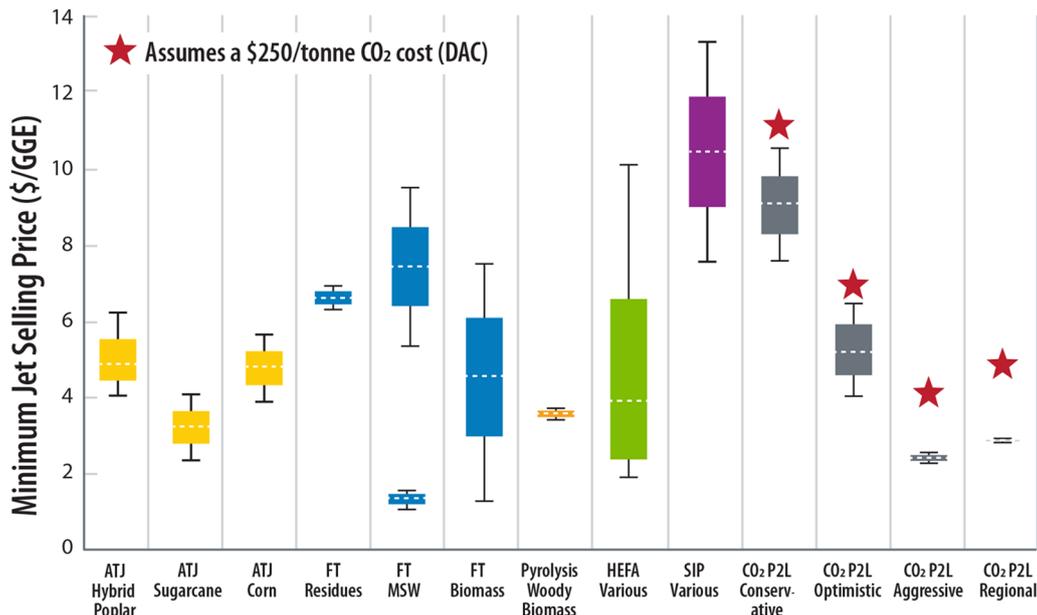*Energy Environ. Sci.*, 2022, **15**, 4798–4812 | **4805**

Fig. 6 Comparison of minimum jet selling price across SAF pathways (FOG = fats, oils, and grease; UCO = used cooking oil). Red stars reflect cost of CO_2-derived SAF if CO_2 price were fixed at $250 per tonne. Data from ref. 51–58.

electrolysis, (3) H_2 generation, (4) balance of plant work and heat, and (5) energy out in the form of SAF. Tabulating these mass and energy flows and multiplying by their respective intensity factors (see Table S9, ESI†) allows for the calculation of total process energy efficiency (EE). Shown in Table 6, we calculate that depending on the CO_2 source and associated energy intensity for purification, the end-to-end energy efficiencies for the as-modeled process ranges from approximately 28–37%. When compared to the energy efficiency reported for other more mature ASTM-certified routes (HEFA, FT, ATJ) we find that all our CO_2-to-SAF cases fell on the lower end for EE. While our best case of using CO_2 sourced from a bioethanol refinery performed similarly to the baseline ATJ and FT cases, all CO_2 cases significantly underperformed HEFA, which showed top end EE values approaching 74%. The top three largest energy sinks in our CO_2-to-SAF processes were H_2 generation for fermentation and hydrotreating at an average of 59% of total energy input, electric demand for CO_2

electrolysis at an average of 21% total energy input, and CO_2 capture + process separations contributing to an average of 20% of the total energy input required. Based on these data, possible avenues for improving the energy efficiency for CO_2-to-SAF moving forward may include minimizing H_2 usage (*e.g.*, through other fermentation stoichiometries), performing electrolysis reactions more efficiently (*e.g.*, lower cell voltages), and minimizing energy demands for CO_2 capture and purification (*e.g.*, one-step reactive capture + conversion).

Region-specific analysis

At the onset of an analysis, it can be unclear precisely when, where, and how a technology would be deployed. Consequently, in the absence of data on commissioning year, country/state of operation, status of the technology, *etc.*, a common first step is the use of averaged global or country-specific economic and technical assumptions, which while useful, can be overly conservative and not necessarily representative of localized opportunities present for the early adopters at a smaller scale. Early adopters will typically seek strategic deployment of assets in these targeted areas with the most favorable economic conditions to raise profit margins and ease the higher cost of pioneer plant deployment. Below we explore possible deployment locations within the United States for early adopters of the CO_2-to-SAF process and highlight notable economic opportunities to produce CO_2-derived SAF at a lower price point.

From the MJSP cost breakdown data presented in Fig. 5, access to a reliable (*i.e.*, high-capacity factor) and cheap source of electricity is expected to be the most significant contributor to the final SAF cost. With most electric grids worldwide still fueled to some degree by fossil resources for the foreseeable future, direct connection to the electrical grid is not considered

Table 6 Calculated energy efficiency and energy intensity values for CO_2-to-SAF based on CO_2 source

CO_2 source	Energy efficiency (%)	Energy intensity (MJ per kg HC fuels)
CO_2 (DAC)	31.5	138.3
CO_2 (DAC, hydroxide)	31.1	140.1
CO_2 (DAC, VTSA)	28.4	153.24
CO_2 cement	33.5	129.9
CO_2 NGCC	35.2	123.5
CO_2 ethanol	36.8	118.3
HEFA FOG[a]	74.0%	59.3
Fischer tropsch[b]	43.6%	101.0
Alcohol-to-jet[c]	39.3%	111.0

[a] Ref. 60. [b] Ref. 61. [c] Ref. 62.

4806 | *Energy Environ. Sci.*, 2022, **15**, 4798–4812

This journal is © The Royal Society of Chemistry 2022

herein nor recommended currently due to the associated high carbon footprint and impact on SAF CI (see Fig. S2, ESI†). Consequently, the first major challenge for P2L CO_2-to-SAF commercialization will be sourcing low-cost renewable electricity. Secondary to the cost of electricity, early adopters of CO_2-to-SAF will also consider the logistics of securing access to a reliable, pure, and cheap source of CO_2. With utility prices subject to supply and demand fluctuations and varying over time, we evaluate current region-specific opportunities based on published United States power purchase agreement (PPA) data for solar and wind derived electricity for the years 2016–2021.[63,64] A PPA represents a contract between an electricity supplier and a consumer where the producer finances the upfront capital, construction, and operating charges, and in return sets a fixed electricity price which the consumer is locked in for a negotiated term of typically 5–20 years. In Table 7, we provide the average negotiated PPA rate for solar and wind energy from 2016–2021, along with the installed capacity for the PPA agreements across the 11 unique operating regions of the U.S. grid shown in Fig. 7 (Hawaii not shown).

Across the regions of the electric grid, we show that on average the lowest cost renewable electricity is provided *via* wind energy in the SPP region at an average price of $0.016 per kW h. Further, SPP also contains the largest PPA-supply of installed wind energy resources at 3918 MW-AC during the period of 2016–2021. While these data only provide an averaged snapshot across the various regions and one-off opportunities for lower electricity pricing may exist in other regions (*e.g.*, SERC-wind, WECC-solar), the combined low price and high supply of wind energy available in the SPP region make for an attractive location for a first-of-a-kind deployment of P2L CO_2-to-SAF.

Within the SPP region most of the installed wind capacity, both PPA and non PPA, is primarily concentrated into two states, Texas and Iowa (see Fig. S3, ESI†), suggesting from the perspective of cost and installed production either of these two states could represent a promising opportunity for P2L CO_2-to-SAF deployment.

For the purposes of this case study we selected Texas as it is also home to some of the largest solar energy projects in the U.S., providing an attractive option to supplement the low-cost wind energy and increase overall capacity factor.[63] Further, Texas
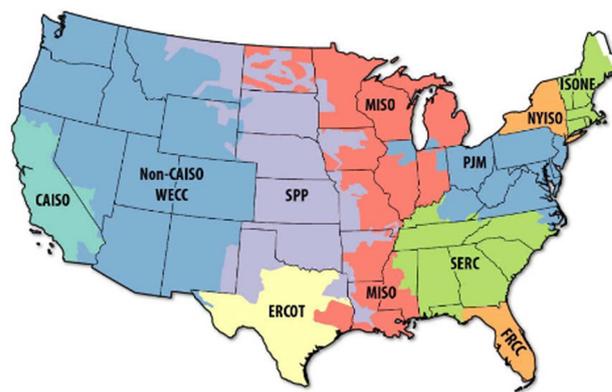

Fig. 7 United States electrical grid operating regions. Reproduced from ref. 65.

offers a diversified selection of CO_2 point sources as well as access to dedicated CO_2 pipeline infrastructure (Fig. S4, ESI†).

From this set of regional economic data we calculate MJSP for the aforementioned LTE and HTE cases, highlighting the opportunity for an early adopter of P2L CO_2-to-SAF specific to the West Texas region. Shown in Fig. 8, under these regional assumptions (full list provided in Table S10, ESI†) we find that the LTE case deployed in the West Texas region could achieve a MJSP of approximately $6.27 per GGE, over $4 cheaper than our default conservative economic scenario which assumes U.S. domestic averaged values. The major driver for the difference in cost is in the assumptions around electricity price which, in the regional economic scenario, is much lower at $0.016 per kW h compared to $0.068 per kW h assumed in the other conservative scenario(s). The regional LTE MJSP is further decreased when considering the application of policy incentives. Applying the low-carbon fuel standard (LCFS) noted above, which provides a financial incentive for fuels sold for use in California, we find that based on the calculated CI for our SAF product of 5 gCO_2e per MJ, the LCFS incentive (based on a credit value assumed here as $171 per ton), is approximately $1.67 per GGE, lowering the MJSP further to $4.60 per GGE (see Fig. S5 for more information, ESI†). Applying the second Inflation Reduction Act (IRA) incentive, we find that, assuming a SAF CI of 5 gCO_2e per MJ, it would offer an additional discount of $1.69 per gal ($1.52 per GGE), bringing the MJSP down to only $3.08 per GGE. Applying the same input cost

Table 7 Average PPA price and installed capacity for U.S. grid regions (2016–2021). Source ref. 63 and 64

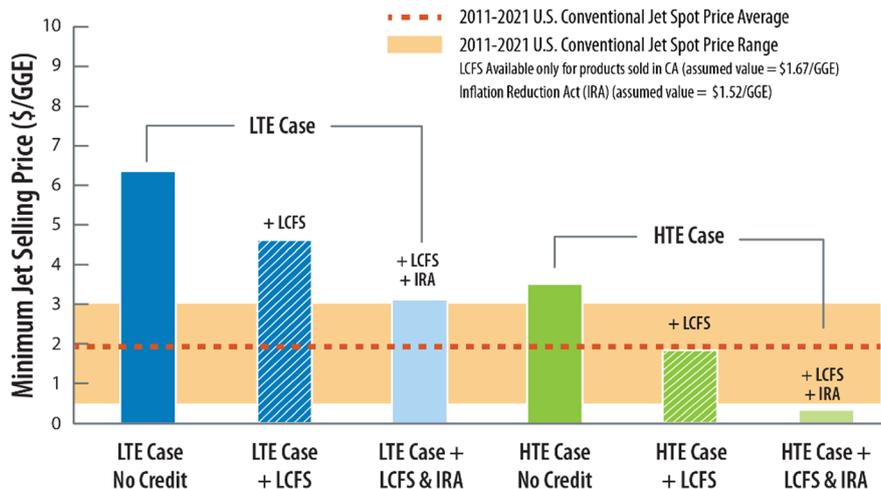| Grid ISO region	Average solar PPA price ($ per kW h)	Installed PPA solar capacity (MW-AC)	Average wind PPA price ($ per kW h)	Installed PPA wind capacity (MW-AC)
CAISO	0.031	1704	0.042	451
ERCOT	0.030	464	0.022	200
FRCC	—	—	—	—
Hawaii	0.095	110	—	—
ISO-NE	0.080	287	0.039	101
MISO	0.038	270	0.023	2888
NYISO	0.098	621	—	—
PJM	0.049	610	0.034	649
SERC	0.034	1332	0.018	479
SPP	0.051	10	0.016	3918
WECC	0.026	4754	0.025	3218

Fig. 8 Regional economic scenario MJSP across case types with and without incentives.

and incentive assumptions to the HTE case, we show the MJSPs range from $3.51 per GGE down to as low as $\sim$\$0.32 per GGE with both incentives. These data suggest that with incentives, pockets of opportunity exist throughout the U.S. and likely abroad in which P2L CO_2-to-SAF processes could be cost-competitive not only with other routes to SAF, but also conventional jet fuel production.

Risks for CO_2-to-SAF commercialization

The development, scale-up, and commercialization of new technologies is often rife with risk. Identifying and mitigating potential risks as early as possible in the commercialization process is critical to increasing the chances of success and long-term viability. With the complete end-to-end CO_2-to-SAF process discussed herein having never been demonstrated previously, we acknowledge the heightened probability for a variety of technical, market, and systems integration risks. To characterize and identify these specific risks, we engaged with a team of subject matter experts with experience across each of the proposed conversion steps as well as technology providers with expertise in process scale up and commercialization. Working with this team, we developed a risk register to characterize risks based on probability and impact to inform and guide future R&D and investments in P2L CO_2-to-SAF. Below we summarize the key takeaways as related to technical, market, and systems integration risks. The full register of risks can be found in Tables S11–S14 (ESI†).

Technical risks. Across the three major conversion steps of electrolysis, syngas fermentation, and catalytic ethanol conversion, the majority of the technical risk was identified in the lower-TRL electrolysis stage(s), specifically for LTE. The proposed risks centered on three elements (1) the relatively small scale of current electrolyzers combined with lack of information on the stability and durability of electrolyzers and the comprising componentry (*e.g.*, membranes and electrocatalysts) at timescales relevant to commercial application, (2) lack of testing on real-world gas compositions (*e.g.*, components found across plant recycle loops and amongst CO_2 point

sources), and (3) the relatively low performance of CO_2 electrolysis systems compared to more mature counterparts (*e.g.*, H_2O electrolysis). The uncertainty around these key performance issues and their impact on process CAPEX, in which electrolyzer unit cost has already been flagged as a key contributor, introduces sizeable risk to the process. Given the relatively high TRL of syngas fermentation and commercial demonstration of that particular step in the process by LanzaTech with over 20 million gallons of ethanol produced from their commercial gas fermentation plant to-date,[66] no significant technical risks were flagged for this step in the process. Similarly, for the thermocatalytic ethanol upgrading, the main identified risks primarily centered on catalyst developmental challenges related to the long term stability and performance metrics. However, on a relative basis the processes of alcohol dehydration, coupling, and oligomerization are well understood and these risks are not anticipated to siginificantly impact process viability given the relatively low cost and carbon footprint associated with replacement of the catalysts.

Market and scaling risks. In addition to the technical risks specific to each conversion step, subject matter experts also commented on broader market risks for CO_2-to-SAF as well as specific risks around scaling the still unproven end-to-end process. From a broader market perspective, subject matter experts identified five key risks for CO_2-to-SAF commercialization: (1) competition for producing intermediate species (*e.g.*, CO, EtOH, olefins) *via* more established processes, (2) sourcing the materials needed to scale the as-designed process (*e.g.*, rare earth metals, membranes, electronics), (3) the high upfront capital cost and loan availability for dedicated energy generation and CO_2 conversion infrastructure, (4) the lack of dedicated CO_2 pipelines and transportation infrastructure, and (5) future allocation preferences of renewable resources (*i.e.*, in the future will CO_2 reduction be the best use of renewable electricity from a climate perspective).

Systems integration risk. A standout feature of the as-modeled CO_2-to-SAF pathway is the combination of three distinct technologies featuring electrolysis, biological fermentation, and thermocatalysis. Harmonizing these disparate technologies within a single continuous process, either standalone or as

4808 | *Energy Environ. Sci.,* 2022, **15**, 4798–4812

This journal is © The Royal Society of Chemistry 2022

Table 8 Linking technical risk to TEA input

Source of risk	TEA variable	Variable range
Unknown durability profile	Electrolyzer replacement interval (years)	1–7
	Electrolyzer replacement fraction (% cost)	5–40
Performance degradation & impact of impurities	LTE voltage (V)	3.0–5.0
	LTE current density (mA cm^{-2})	100–500
	ETJ catalyst price increase (%)	0–100
	ETO conversion rate (%)	70–98
Difficulty in finding investors	Loan interest rate (%)	8.0–12.0
Handling process turndown and intermittency	Capacity factor (%)	70–90
Availability of critical components	LTE capital cost ($ per m^2)	15 000–22 000

part of a larger and more integrated process raises risks around systems integration. In linking three unique conversion technologies under one end-to-end process (Fig. 2), subject matter experts identified three major systems integration risks/challenges: (1) managing the intermittency of input electricity and/or managing process turndowns and how to size the supporting biological and thermocatalytic conversion steps to maximize capacity factor, (2) as-designed the process may be overly complex, involving technologies sufficiently different as to require specific expertise for each operation, and (3) lack of opportunities for process intensification and modularity.

Connecting risk to techno-economics. The risk register developed from subject matter expert feedback (Tables S10–S13, ESI†) suggests that despite choosing moderately high TRL individual conversion technologies, when all combined, the as-designed process faces several potentially high-severity risks that warrant further focus and R&D. Most identified risks were technical in nature and skewed toward the electrolysis stage(s) which are comparatively the lowest TRL piece(s) of the process. To evaluate how the identified process risks may influence MJSP, we translated, where possible, the aforementioned risks into input parameters for the LTE case techno-economic model (Table 8) and analysed the impact on MJSP. Shown in Fig. 9, we find that uncertainty around the performance degradation of key process metrics (e.g., current density, capacity factor, ethanol to olefins (ETO) conversion) significantly affects MJSP,

on the order of up to ~10–40% depending on the specific metric. The cost and interval in which the electrolysis componentry is replaced is also seen as having a large impact on the underlying TEA, varying MJSP by up to ~10% each. Continuing R&D efforts into these key technical areas will be critical to reducing uncertainty and lowering process risk to allow for more accurate predictions of MJSP.

Considerations for the future. As the number of new technology offerings grow in the future and additional routes to SAF and other products are identified, it will be critically important to evaluate these processes using consistent assumptions to help the field move forward. If assumptions are not held constant across analyses and rather vary between laboratories, countries, or international agencies as in the past, progress will continue to be clouded and slowed. Maintaining full transparency of assumptions with the goal of harmonizing life cycle assumptions in particular will be critical, as herein we identified inconsistencies across two of the major LCA databases and literature sources, impacting the final and relative ranking of SAF CI values.

Although much of the technological foundation has been laid for P2L CO$_2$-to-SAF, major research and development is still needed, particularly on the electrolysis stage(s) and general process intensification. Scaling the production of electrolyzers to drive down unit costs (and size) while running concurrent long term testing to evaluate and identify failure mechanisms are two top R&D needs to design and build systems capable of competing commercially. Further, with renewable energy utilization being a cornerstone of P2L, more research is needed to understand the impacts of intermittency and specifically on how to buffer individual processes, each with their own unique technology elements (e.g., electro-, bio-, and thermo-chemistry), during system turndowns. Finally, and more broadly, there is a need for systems analysis and systems of systems analysis which considers not only the standalone process, but evaluates how such a P2L process would play a part within a network of larger energy systems across the grid as the penetration of renewable electricity continues to expand around the globe.

Conclusion

In this study, the techno-economic and life cycle merits of an emerging P2L CO$_2$-to-SAF pathway were evaluated and compared against several ASTM-approved SAF production routes.
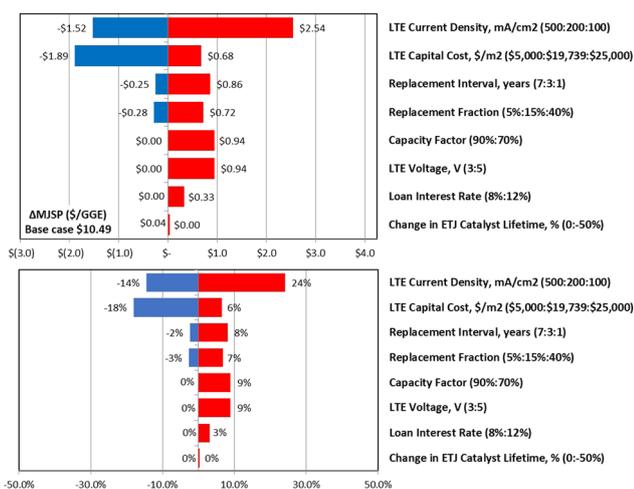

Fig. 9 Linking risks to the minimum jet fuel selling price.

This journal is © The Royal Society of Chemistry 2022

Energy Environ. Sci., 2022, **15**, 4798–4812 | **4809**

Our analysis shows P2L CO_2-to-SAF can be an attractive future option for SAF production being competitive both in terms of costs and CI, providing a diversified and complementary option for the conversion of CO_2 to SAF beyond the decades old MTO and FT technologies. When compared to petroleum jet fuel, the models and analysis presented herein indicate that currently CO_2-to-SAF is more costly and that the gap can be reduced, but not fully closed, by pursuing high-efficiency, high-yield technologies in locations with access to low-cost renewable electricity. Under the most aggressive economic scenario considered, we find that with advancements to the underlying technologies combined with substantial reductions in the price of electricity down to $0.01 per kW h, SAF costs as low as $2.25–2.53 per GGE may be obtainable in the future without incentives. Specific to the United States, our analysis suggests that near-term deployment of P2L CO_2-to-SAF in the West Texas region could see production costs as low as $3.51 per GGE using currently available technology, with the potential for MJSPs as low as $0.32 per GGE driven by $3.19 per GGE total applied incentives ($1.67 from LCFS and $1.52 from the Inflation Reduction Act). Producing SAF from CO_2 is expected to lower the CI of the fuel by 50–94% relative to fossil jet fuel, similar to other SAF production methods. Further minimizing SAF CI will rely on sourcing high purity CO_2 feedstocks, the utilization of low energy intensity conversion pathways, and by ensuring that front-end CO_2 capture and purification stages are fully integrated with renewable energy sources.

Abbreviations

ACCE	Aspen capital cost estimator
AEM	Anion-exchange membrane
ASTM	American society for testing and materials
ATJ	Alcohol-to-jet
BBL	Barrel
CAPEX	Capital expense
CI	Carbon intensity
CO	Carbon monoxide
CO2e	CO2 equivalent
DAC	Direct air capture
ETO	Ethanol-to-olefins
EtOH	Ethanol
FE	Fossil energy
FOG	Fats, oils, and greases
FT	Fischer-tropsch
GGE	Gallon of gasoline equivalent
GREET	Greenhouse gases, regulated emissions, and energy use in technologies model
HEFA	Hydroprocessed esters and fatty acids
THE	High-temperature electrolysis
IEA	International energy agency
LCA	Life cycle analysis
LCFS	Low-carbon fuel standard
LTE	Low-temperature electrolysis
MJSP	Minimum jet fuel selling price
MSW	Municipal solid waste
MTO	Methanol to olefins
NGCC	Natural gas combined cycle
P2L	Power-to-liquids
PNNL	Pacific northwest national laboratory
PPA	Power purchase agreement
PTW	Pump-to-wake
SAF	Sustainable aviation fuel
SOEC	Solid-oxide electrochemical cell
SPK	Synthetic paraffinic kerosene
SSA	Sustainable skies act
TEA	Techno-economic analysis
VTS	Vacuum temperature swing
WTP	Well-to-pump
WTWa	Well-to-wake

Conflicts of interest

There are no conflicts to declare.

Acknowledgements

References

1 The International Civil Aviation Organization, The World of Air Transport in 2019, https://www.icao.int/annual-report-2019/Pages/the-world-of-air-transport-in-2019.aspx, (accessed 12/14, 2021).

2 IEA, Transport sector CO2 emissions by mode in the Sustainable Development Scenario, 2000-2030, https://www.iea.org/data-and-statistics/charts/transport-sector-co2-emissions-by-mode-in-the-sustainable-development-scenario-2000-2030, (accessed 12/14, 2021).

3 IEA, Tracking Aviation 2020, https://www.iea.org/reports/tracking-aviation-2020, (accessed 12/14, 2021).

4 ICF, Fueling Net Zero: How the aviation industry can deploy sufficient sustainable aviation fuel to meet climate demands, https://www.icf.com/insights/transportation/deploying-sustainable-aviation-fuel-to-meet-climate-ambition, (accessed 12/14, 2021).

5 U.S. Department of Energy, Sustainable Aviation Fuel: Review of Technical Pathways, https://www.energy.gov/

4810 | Energy Environ. Sci., 2022, 15, 4798–4812

This journal is © The Royal Society of Chemistry 2022

sites/prod/files/2020/09/f78/beto-sust-aviation-fuel-sep-2020. pdf, (accessed 12/14, 2021).

6 IEA, Energy Technology Perspectives 2020, https://www.iea. org/reports/energy-technology-perspectives-2020, (accessed 12/14, 2021).

7 M. Bailera, P. Lisbona, L. M. Romeo and S. Espatolero, *Renewable Sustainable Energy Rev.*, 2017, **69**, 292–312.

8 A. Buttler and H. Spliethoff, *Renewable Sustainable Energy Rev.*, 2018, **82**, 2440–2454.

9 R. G. Grim, Z. Huang, M. T. Guarnieri, J. R. Ferrell, L. Tao and J. A. Schaidle, *Energy Environ. Sci.*, 2020, **13**, 472–494.

10 P. Schmidt, V. Batteiger, A. Roth, W. Weindorf and T. Raksha, *Chem. Ing. Tech.*, 2018, **90**, 127–140.

11 A. Alam, M. F. H. Masum and P. Dwivedi, *GCB Bioenergy*, 2021, **13**, 1800–1813.

12 A. Diniz, R. Sargeant and G. J. Millar, *Biotechnol. Biofuels*, 2018, **11**, 161.

13 P. Laveille, J. Uratani, J. G. G. Barron, M. Brodeur-Campbell, N. R. Chandak, A. George, S. Morin, A. R. Galvan and M. Berthod, *Biofuels, Bioprod. Biorefin.*, 2021, **16**(1), 27–42.

14 R. Shen, L. Tao and B. Yang, *BioFPR*, 2019, **13**, 486–501.

15 A. H. Tanzil, K. Brandt, M. Wolcott, X. Zhang and M. Garcia-Perez, *Biomass Bioenergy*, 2021, **145**, 105942.

16 A. H. Tanzil, X. Zhang, M. Wolcott, K. Brandt, C. Stöckle, G. Murthy and M. Garcia-Perez, *Biomass Bioenergy*, 2021, **146**, 105937.

17 W.-C. Wang and L. Tao, *Renewable Sustainable Energy Rev.*, 2016, **53**, 801–822.

18 S. Geleynse, K. Brandt, M. Garcia-Perez, M. Wolcott and X. Zhang, *ChemSusChem*, 2018, **11**, 3728–3741.

19 D. Silva Braz and A. Pinto Mariano, *Bioresour. Technol.*, 2018, **268**, 9–19.

20 Y. Chen, C. W. Li and M. W. Kanan, *J. Am. Chem. Soc.*, 2012, **134**, 19969–19972.

21 B. Kim, S. Ma, H.-R. Molly Jhong and P. J. A. Kenis, *Electrochim. Acta*, 2015, **166**, 271–276.

22 K. P. Kuhl, E. R. Cave, D. N. Abram and T. F. Jaramillo, *Energy Environ. Sci.*, 2012, **5**, 7050–7059.

23 Z. Liu, H. Yang, R. Kutz and R. I. Masel, *J. Electrochem. Soc.*, 2018, **165**, J3371–J3377.

24 R. Kungas, P. Blennow, T. Heiredal-Clausen, T. H. Norby, J. Rass-Hansen, J. B. Hansen and P. G. Moses, *ECS Trans.*, 2019, **91**, 215–223.

25 C. Mittal, C. Hadsbjerg and P. Blennow, *Chem. Eng. World*, 2017, 44–46.

26 R. Küngas, *J. Electrochem. Soc.*, 2020, **167**(4), 044508.

27 C. Duan, R. Kee, H. Zhu, N. Sullivan, L. Zhu, L. Bian, D. Jennings and R. O'Hayre, *Nat. Energy*, 2019, **4**, 230–240.

28 E. Jeng and F. Jiao, *Reaction Chem. Eng.*, 2020, **5**, 1768–1775.

29 NREL, H2A: Hydrogen Analysis Production Models, https://www.nrel.gov/hydrogen/h2a-production-models.html, (accessed 03/19, 2021).

30 K. Xie, Y. Zhang, G. Meng and J. T. S. Irvine, *J. Mater. Chem.*, 2011, **21**, 195–198.

31 F. Liew, M. E. Martin, R. C. Tappel, B. D. Heijstra, C. Mihalcea and M. Kopke, *Front. Microbiol.*, 2016, **7**, 694.

32 LanzaTech, CCU-Now: fuels and chemicals from waste, (https://ec.europa.eu/energy/sites/ener/files/documents/25_sean_simpson-lanzatech.pdf).

33 R. M. Handler, D. R. Shonnard, E. M. Griffing, A. Lai and I. Palou-Rivera, *Ind. Eng. Chem. Res.*, 2015, **55**, 3253–3261.

34 V. L. Dagle, A. D. Winkelman, N. R. Jaegers, J. Saavedra-Lopez, J. Hu, M. H. Engelhard, S. E. Habas, S. A. Akhade, L. Kovarik, V.-A. Glezakou, R. Rousseau, Y. Wang and R. A. Dagle, *ACS Catal.*, 2020, **10**, 10602–10613.

35 M. A. Lilga, R. T. Hallen, K. O. Albrecht, A. R. Cooper, J. G. Frye and K. K. Ramasamy, *US Pat.*, 9771533B2, 2017.

36 U.S. Department of Energy, Office of Energy Efficiency and Renewable Energy, Hydrogen Production: Electrolysis, https://www.energy.gov/eere/fuelcells/hydrogen-production-electrolysis, (accessed 12/17, 2021).

37 Z. Huang, G. Grim, J. Schaidle and L. Tao, *Appl. Energy*, 2020, **280**, 115964.

38 LanzaTech, World's First Commercial Waste Gas to Ethanol Plant Starts Up, https://www.lanzatech.com/2018/06/08/worlds-first-commercial-waste-gas-ethanol-plant-starts/, (accessed 1/3, 2022).

39 NREL, Current Central Hydrogen Production from Polymer Electrolyte Membrane (PEM) Electrolysis (2019) version 3.2018, https://www.nrel.gov/hydrogen/assets/docs/current-central-pem-electrolysis-v3-2018.xlsm, (accessed 09/30, 2022).

40 U.S. Department of Energy, Office of Energy Efficiency and Renewable Energy, Hydrogen Shot, https://www.energy.gov/eere/fuelcells/hydrogen-shot, (accessed 1/3, 2022).

41 Argonne National Laboratory, GREET WTW Calculator, https://greet.es.anl.gov/tools, (accessed 1/3, 2022).

42 N. von der Assen, L. J. Muller, A. Steingrube, P. Voll and A. Bardow, *Environ. Sci. Technol.*, 2016, **50**, 1093–1101.

43 M. M. J. de Jonge, J. Daemen, J. M. Loriaux, Z. J. N. Steinmann and M. A. J. Huijbregts, *Int. J. Greenhouse Gas Control*, 2019, **80**, 25–31.

44 S. Deutz and A. Bardow, *Nat. Energy*, 2021, **6**, 203–213.

45 J. Burkhardt, A. Patyk, P. Tanguy and C. Retzke, *Appl. Energy*, 2016, **181**, 54–64.

46 V. Fthenakis and E. Leccisi, *Prog. Photovoltaics Res. Appl.*, 2021, **29**, 1068–1077.

47 T. G. Deutsch, S. Baker, P. Agbo, D. R. Kauffman, J. Vickers and J. A. Schaidle, Summary Report of the Reactive CO2 Capture: Process Integration for the New Carbon Economy Workshop, https://www.nrel.gov/docs/fy21osti/78466.pdf, (accessed 1/3, 2022).

48 Argonne National Laboratory, GREET.Net: A fresh design for GREET life cycle analysis tool, https://greet.es.anl.gov/index.php?content=greetdotnet, (accessed 1/03, 2022).

49 California Air Resource Board, Weekly LCFS Credit Transfer Activity Reports, https://www.arb.ca.gov/fuels/lcfs/credit/lrtweeklycreditreports.htm, (accessed 12/15, 2021).

50 J. A. Yarmuth 117th Congress, H.R.5376 - Inflation Reduction Act of 2022, https://www.congress.gov/bill/117th-congress/house-bill/5376, (accessed 09/30, 2022).

51 J. T. Crawford, C. W. Shan, E. Budsberg, H. Morgan, R. Bura and R. Gustafson, *Biotechnol. Biofuels*, 2016, **9**, 141.

This journal is © The Royal Society of Chemistry 2022

Energy Environ. Sci., 2022, **15**, 4798–4812 | 4811

52 S. de Jong, R. Hoefnagels, A. Faaij, R. Slade, R. Mawhood and M. Junginger, *Biofuels, Bioprod. Biorefin.*, 2015, **9**, 778–800.

53 B. C. Klein, M. F. Chagas, T. L. Junqueira, M. C. A. F. Rezende, T. D. F. Cardoso, O. Cavalett and A. Bonomi, *Appl. Energy*, 2018, **209**, 290–305.

54 U. Neuling and M. Kaltschmitt, *Fuel Process. Technol.*, 2018, **171**, 54–69.

55 M. F. Shahriar and A. Khanal, *Fuel*, 2022, **325**, 124905.

56 R. Shen, L. Tao and B. Yang, *Biofuels, Bioprod. Biorefin.*, 2018, **13**, 486–501.

57 O. Winjobi, D. R. Shonnard and W. Zhou, *ACS Sustainable Chem. Eng.*, 2017, **5**, 4529–4540.

58 Z. Yang, K. Qian, X. Zhang, H. Lei, C. Xin, Y. Zhang, M. Qian and E. Villota, *Energy*, 2018, **154**, 289–297.

59 EIA, U.S. Gulf Coast Kerosene-Type Jet Fuel Spot Price FOB, **https://www.eia.gov/dnav/pet/hist/eer_epjk_pf4_rgc_dpgD.htm**, (accessed 3/15/2022, 2022).

60 L. Tao, A. Milbrandt, Y. Zhang and W. C. Wang, *Biotechnol. Biofuels*, 2017, **10**, 261.

61 Y. Zhang, A. H. Sahir, E. C. D. Tan, M. S. Talmadge, R. Davis, M. J. Biddy and L. Tao, *Green Chem.*, 2018, **20**, 5358–5373.

62 L. Tao, J. N. Markham, Z. Haq and M. J. Biddy, *Green Chem.*, 2017, **19**, 1082–1101.

63 M. Bolinger, J. Seel, C. Warner and D. Robson, Utility-Scale Solar, 2021 Edition, **https://emp.lbl.gov/utility-scale-solar**, (accessed 1/5, 2022).

64 R. Wiser, M. Bolinger, B. Hoen, D. Millstein, J. Rand, G. Barbose, N. Darghouth, W. Gorman, S. Jeong, A. Mills and B. Paulos, Land-Based Wind Market Report: 2021 Edition, **https://emp.lbl.gov/wind-technologies-market-report/**, (accessed 1/5, 2022).

65 P. Denholm, Y. Sun and T. Mai, An Introduction to Grid Services: Concepts, Technical Requirements, and Provision from Wind, **https://www.nrel.gov/docs/fy19osti/72578.pdf**, (accessed 1/5, 2022).

66 LanzaTech, Carbon Engineering and LanzaTech partner to advance jet fuel made from air, **https://www.lanzatech.com/2021/07/26/carbon-engineering-and-lanzatech-partner-to-advance-jet-fuel-made-from-air/**, (accessed 1/5, 2022).